A Hybrid Constrained Genetic Algorithm / Particle Swarm Optimisation Load Flow Algorithm

T. O. Ting, K. P. Wong, and C. Y. Chung

Computational Intelligence Applications Research Laboratory,

Department of Electrical Engineering,

The Hong Kong Polytechnic University, Hung Hom, Kowloon, Hong Kong

{chan.xiuyan, eekpwong, eecychun}@polyu.edu.hk

Abstract: This paper develops a hybrid Constrained Genetic Algorithm and Particle Swarm Optimisation method for the evaluation of the load flow in heavy-loaded power systems. The new algorithm is demonstrated by its applications to find the maximum loading points of three IEEE test systems. The paper also reports the experimental determination of the best values of the parameters for use in the Particle Swarm Optimisation part of the hybrid algorithm.

1 Introduction

Over the previous decades numerous techniques have been developed to determine the loadability limits of power systems. One class of methods utilizes the distance between the operating load-flow solution and bifurcation point of a system [1, 2]. Yet another class of methods investigates the voltage stability limits based upon different types of load-flow analysis [3, 4], energy methods [5] and sensitivity analysis [6, 7]. Works in [8, 9] utilize the minimum singular value of the Jacobian matrix as a voltage stability index. The maximum loading point (MLP) is estimated in [10] by using a set of stable operating point which is based on the analysis of Jacobian matrix behaviour. Meanwhile, continuation methods are widely known as very powerful, though slow, methods to estimate the system maximum loading [11]. Apart from the above methods, load flow study still remains a very important approach in checking on the maximum loading point of a power system.

Efficient and reliable load flow solutions, such as the Newton-Raphson (NR) [12] and the fast decoupled load flow [13], have been widely used by the power industry. However, when a power system becomes highly stressed, it will be difficult for conventional methods to converge. Also the employment of Flexible AC transmission system (FACTS) devices will introduce more non-linear

elements into the power network and weakens the performance of conventional load flow approaches because of the more nonlinear load flow equations. In coping with the nonlinearity of the load models, a critical evaluation of step size optimisation based load flow methods is proposed in [14] for ill-conditioned, heavily loaded and overloaded systems. However, this method is highly sensitive to the initial settings of the variables.

Load flow methods based on evolutionary computation have also been proposed. Their solution process does not rely on the starting values of the variables. A Constrained Genetic Algorithm (CGA) load flow method was reported in [15] and its robustness and efficiency was enhanced using the concept of virtual population and solution acceleration techniques developed in [16]. The enhanced CGA is referred to as the Advanced Constrained Genetic Algorithm (ACGA) load flow algorithm. The solution acceleration techniques in ACGA consist of the nodal voltage differential technique and the gradient acceleration technique. The ACGA algorithm has been found to have the capability to determine both the normal and abnormal load flow solutions of a number of IEEE test systems. It has also been found that ACGA can determine the load flow solution at the maximum power loading point with only a few iterations. While the details of ACGA can be found in [16], the framework of the ACGA is shown here in Fig. 1. In this framework, a virtual population consists of the current population of candidate load flow solutions and two new populations, A and B, derived from the current population using the nodal voltage differential solution acceleration method. Population A is derived by accelerating candidate solutions in the current population towards the best candidate solution in the same population. On the other hand, population B is formed by accelerating candidate solutions away from the best candidate solution in the population. The current population, population A and population B are then combined to form population C. The resultant population is formed from population C with twenty-five percent of its candidate solutions accelerated by means of the gradient technique. The resultant population is then used as the current population in the evolutionary cycle.

It can be observed that the nodal voltage differential acceleration technique employed in ACGA is not general enough. This technique only upgrades the candidate solutions in two opposite directions. But there is no guarantee that upgrading along these directions will help the evolutionary optimisation process. In the present work, it is proposed to employ the Particle Swarm Optimisation (PSO) technique [17] to replace the nodal voltage differential acceleration technique in ACGA as shown in Fig. 2, because the PSO can upgrade the candidate solutions in many different directions and hence

cover a bigger search space than the voltage differential acceleration method. The use of PSO here can also be viewed as a method of mutation in the genetic algorithm process. Hence, to prevent any good candidate solutions from being destroyed by the PSO technique, the technique is only applied subject to a 'mutation probability' setting as indicated by *mp*% in Fig. 2. With this arrangement, the resultant algorithm can be viewed as a hybrid CGA/PSO algorithm for solving the load flow problem. Because of the more general nature of the hybrid algorithm, it should be more powerful than its predecessor ACGA and should be capable of obtaining better load flow solution values particularly when the power system is very heavily loaded. It is, however, emphasized here that the new algorithm is a powerful alternative when conventional methods fail to find the load flow solution. It is also noted here that although PSO has been used in solving power system optimisation problems [18-21], it has not been employed in the way described in this paper.

This paper reports work on the development of a hybrid CGA/PSO algorithm for finding load flow solutions. The earlier work in [26], developed a Two-phase PSO algorithm to solve the load flow problem. The Two-phase PSO algorithm is very much different from the proposed hybrid algorithm proposed in this paper. Furthermore, in the work in [26], the PSO algorithm is run simultaneously in two sets, which has different parameter setting for each set. The work in [26] provides some preliminary insights in tuning the parameters with regards to solving load flow problem. Subsequent to [26], the further work in [27] hybridizes PSO with GA, forming a hybrid Evolutionary Algorithm in the aim of locating Type-1 load flow solutions. The framework of the hybrid algorithm in [27] is in its infancy stage. This framework is then enhanced and refined in the present work with optimal order of manipulating operators, as depicted in Fig. 2. In addition, in the present paper, all the PSO parameters are investigated empirically through parameter sensitivity analysis to determine the optimal set of parameter settings. Thus in the present paper, a comprehensive PSO parameter analysis is presented and results are analyzed in terms of accuracy, speed and stability. Another distinct aspect of the present paper is the application of the proposed hybrid algorithm to determine the maximum loading points of highly stressed power systems. The application studies show significant improvements by the proposed hybrid algorithm when compared to those obtained using ACCA in [16].

In the PSO methods, there are several parameters to be set. In order to use the PSO efficiently, the value ranges of these parameters should be investigated for solving the load flow problem. The paper also describes the experimental approach and parametric sensitivity analyses in finding the appropriate

value ranges of the PSO parameter settings. The power of the new hybrid algorithm is demonstrated by the application of the new algorithm to determine the maximum power loading points of three IEEE test systems.

2 Load Flow Problem Formulation

In an interconnected n node power system, there are N_{PQ} load nodes, N_{PV} voltage-controlled nodes and one slack bus. In rectangular coordinates, there are 2(n-1) unknowns to find. These unknowns are the voltages of the load nodes, the voltage angles and the reactive power at the generator nodes. The load flow problem in this paper can be formulated as nonlinear optimisation problem [15] that is the minimisation of the objective function resulting from the summation of squares of the power mismatches and voltage mismatches. At any node i the nodal active power, P_i and reactive power, Q_i are given as follows:

$$P_i = E_i \sum_{j=1}^{n} (G_{ij}E_j - B_{ij}F_j) + F_i \sum_{j=1}^{n} (G_{ij}F_j + B_{ij}E_j) \tag{1}$$

$$Q_i = F_i \sum_{j=1}^{n} (G_{ij}E_j - B_{ij}F_j) - E_i \sum_{j=1}^{n} (G_{ij}F_j + B_{ij}E_j) \tag{2}$$

where G_{ij} and B_{ij} are the $(i, j)th$ element of the admittance matrix. E_i and F_i are real and imaginary part of the voltage at node i. If node i is a PQ-node where the load demand is specified, then the mismatches in active and reactive powers, ΔP_i and ΔQ_i respectively, are given by:

$$\Delta P_i = \left| P_i^{sp} - P_i \right| \tag{3}$$

$$\Delta Q_i = \left| Q_i^{sp} - Q_i \right| \tag{4}$$

in which P_i^{sp} and Q_i^{sp} are the specified active and reactive powers at node i. When node i is a PV-node, the magnitude of the voltage, V_i^{sp} and the active power generation at node i are specified. The mismatch in voltage magnitude at node i can be defined as:

$$\Delta V_i = \left| V_i^{sp} - V_i \right| \tag{5}$$

In eqn. (5), V_i is the calculated nodal voltage at PV-node i and is given by:

$$V_i = \sqrt{E_i^2 + F_i^2} \tag{6}$$

Apart from solving the load flow problem by the conventional methods, the problem can be viewed as an optimisation problem, in which an objective function H is to be minimised:

$$H = \sum_{i \in N_{pq}+N_{pv}} \Delta P_i^2 + \sum_{i \in N_{pq}} \Delta Q_i^2 + \sum_{i \in N_{pv}} \Delta V_i^2 \quad (7)$$

where N_{pq} and N_{pv} are the total numbers of PQ- and PV-nodes respectively. When the load flow problem is solvable, the value of H is zero or in the vicinity of zero at the end of the optimisation process. If the problem is unsolvable, the value of H will be greater than zero.

In the minimisation process, the fitness or the degree of goodness of the particle as a candidate solution is measured by means of the following fitness function F [16]:

$$F = \frac{1}{10^{-5} + 2H - H_{av}} \quad (8)$$

where H_{av} is the average of mismatches representing the measure of the evenness of the spread of mismatch values throughout the nodes and is calculated from:

$$H_{av} = \frac{\sum_{i=2}^{n} \Delta P_i}{n_{pv} + n_{pq}} + \frac{\sum_{i \in n_{pq}} \Delta Q_i}{n_{pq}} \quad (9)$$

3 Particle Swarm Optimisation Method

As Genetic Algorithm is now well-known and the details of the Constrained Genetic Algorithm for load flow can be found in references [15] and [16], only the Particle Swarm Optimisation (PSO) method [17] is described in this paper. The method has been found to be able to solve optimisation problems featuring non-differentiability, high dimension, multiple optima and non-linearity. The PSO algorithm mimics the movement of individuals such as fishes, birds, or insects within a group or swarm. Similar to GA, a PSO consists of a population refining its knowledge of the given search space. PSO is inspired by particles moving around in the search space. The individuals in a PSO thus have their own positions and velocities.

Instead of using evolutionary operators such as selection, mutation and crossover, each particle in the population moves in the search space with velocity which is dynamically adjusted. Each particle moves in the search space with velocity which is dynamically adjusted and balanced based on its own best movement (*pbest*) and the best movement of the group (*gbest*). In PSO, a population consists of N particles. Each particle has d variables (dimensions) and each variable has its own range of value, velocity and position. The velocities and positions are updated every iteration until maximum iteration is reached. The particle keeps track of its coordinates in the search space, which are associated with

the best solution it has achieved so far. This value is known as *pbest*. Another best value that is tracked is the overall best value or the best solution, *gbest*, in the population.

As stated, the PSO technique consists of, at each time step, changing the velocity of each particle toward its *pbest* and *gbest* solutions. The movement is weighted by a random term, with separate random numbers being generated toward *pbest* and *gbest* values. For example the *i*th particle consisting *d* dimensions is represented as $X_i = (X_{i,1}, X_{i,2}, X_{i,3}, \ldots, X_{i,d})$. The same notation applied to the velocity, $V_i = (V_{i,1}, V_{i,2}, V_{i,3}, \ldots, V_{i,d})$. The best previous position of the *i*th particle is recorded and represented as $pbest_i = (pbest_{i,1}, pbest_{i,2}, pbest_{i,3}, \ldots pbest_{i,d})$. For minimisation, the value of $pbest_i$ with lowest fitness is taken to be *gbest*. The modification of velocity and position are calculated using the current velocity and the distance from $pbest_{i,j}$ to $gbest_j$ as in:

$$V_{i,j}^{t} = wV_i^{t-1} + \rho_1 r_1 (gbest_j - X_{i,j}^{t-1}) + \rho_2 r_2 (pbest_{i,j} - X_{i,j}^{t-1}) \quad (10)$$

$$X_{i,j}^{t} = X_{i,j}^{t-1} + V_{i,j}^{t} \quad (11)$$

where $i \in 1...N, j \in 1...d, t \in 1...T$ with N is the number of population size, d is the number of dimension and T is the number of maximum generation. The parameters ρ_1 and ρ_2 are set to constant values, which are normally given as 2.0 whereas r_1 and r_2 are two random values, uniformly distributed in [0, 1]. The constants ρ_1 and ρ_2 represent the weighting of the stochastic acceleration terms that pull each particle toward *pbest* and *gbest* positions.

The position X of each particle is updated for every dimension for all particles in each iteration. This is done by adding the velocity vector to the position vector, as described in eqn. (11) above. In eqn. (10), w is known as the inertia weight [22]. Suitable selection of w provides a balance between global and local explorations, thus requiring less iteration on average to find sufficiently optimal solution. Low values of w limits the contribution of the previous velocity to the new velocity, limiting step sizes and therefore, limiting exploration. On the other hand, high values result in abrupt movement toward target regions. When applying PSO to the load flow problem, each particle is a candidate solution whereby the elements are the unknown real and imaginary parts of the power network nodal voltages.

4 Proposed Hybrid Constrained GA/PSO Load Flow Algorithm

As described in the introduction section, the proposed hybrid CGA/PSO algorithm for load flow is to replace the nodal voltage differential technique in the ACGA algorithm by PSO, which is triggered on when the mutation probability value is higher than the preset *mp*% as shown in Fig. 2. The procedure of the proposed hybrid algorithm is given in the following:

1. Initialize the particles, consisting of the real and imaginary parts of the nodal voltages of the candidate solutions in the population.
2. Evaluate the fitness of all particles using eqn (8).
3. Generate new population of candidate solutions using roulette-wheel selection, 2-point crossover and PSO mutation.
4. Perform the constraint satisfaction process on the candidate solutions in the new population for the generator nodes and load nodes as described in [15].
5. Accelerate 25% of the constrained candidate solutions using the gradient technique in [16].
6. Update the best solution.
7. Go to step 2 until the termination criterion is met.

In step 3 above, the PSO algorithm is applied as a mutation strategy. The optimal mutation probability is found through parameter sensitivity analysis in section 6.3. The algorithm will terminate when the power mismatches of the PQ nodes and the power and voltage mismatches of the PV nodes are within the preset power and voltage mismatch tolerances, otherwise it will terminate on reaching the maximum allowable number of evolutionary generations. This termination criterion is employed in step 7 of the above procedure.

5 Parameter Settings of PSO

PSO has several parameters, which are the number of particles in the swarm (N), inertia weight (w), maximum velocity (V_{max}), the parameter for attraction towards *pbest* and *gbest* (ρ_1 and ρ_2). In this work, the parameters ρ_1 and ρ_2 are set to constant values, which are commonly set as 2.0. The constants, ρ_1 and ρ_2 represent the weighting of the stochastic acceleration terms that pull each particle toward *pbest* and *gbest* positions, acting as the cognitive and social parameters respectively. The r_1 and r_2 are two random values, uniformly distributed in [0, 1]. To prevent any undesirable exploration of a

particle along a given dimension, the velocity may be restricted by a constriction coefficient [23] but this yields negative effects [24]. Instead of using a constriction coefficient, the velocity in a dimension is restricted by the maximum velocity (V_{max}). This keeps the random search of potential solutions within control. The value of V_{max} in this work is 10% of the search range, which is the best value from parameter sensitivity analysis. Other parameters such as inertia weight (w) and population size (N) are found from the parameter sensitivity analysis presented in the following section. The initial settings of the parameters are as shown in Tables 1 and 2.

6 Parameter Sensitivity Analysis in Hybrid CGA/PSO

In determining the inertia weight (w), population size (N) and the mutation probability, mp, by sensitivity analysis for the proposed hybrid algorithm, the IEEE 30-, 57- and 118-bus systems are used [25] and the algorithm is run with different parameter settings. The settings given in Tables 1 and 2 are applied to all the experiments unless otherwise noted in the sub-section below. The algorithm is executed on a 3.0 GHz Pentium IV computer. The results of these experiments will be presented in tables with the column containing the attributes as follows:

Ave Time : Average time taken to complete a trial. Only successful trials are considered.

Ave Iter : The average iteration for a trial which is successful.

S.R. : Success rate. A trial is considered successful if all nodes value is within the tolerance before maximum generation, T is reached.

Std Dev : This is standard deviation. A small standard deviation denotes that the algorithm is stable.

Best : The best results obtained within all successful trials.

Average : Average of all trials. Only successful trials are taken into account.

Worst : The worst result among all successful trials

6.1 Effect of Inertia Weight (w) in PSO Equations

The value of inertia weight, w is in the range of 0 to 1. In determining the best value of w for the load flow problem w is varied from 0.1 until 0.9 with a step increment of 0.1 as shown in Fig. 3. In this figure, the case of IEEE 118-bus system is illustrated. The numerical results are tabulated in Table 3 and illustrated by the relevant curves in Fig. 3, representing the average iteration, average time and

success rate. From this graph, the average time and average iteration increase with respect to higher value of *w* while at the same time, the success rate decreases. In other words, the success rate (S.R.) deteriorates as the value of inertia weight increases. It seems that smaller value of *w* is more efficient as this guarantees better reliability and cheaper computational cost. Therefore, *w*=0.1 is adopted as the best setting for future analysis, highlighted in Table 3 below. The similar analysis has been carried out on IEEE 30- and 57- bus systems. The same value for *w* is concluded in both analyses, depicted in Table 4.

6.2 Effect of Population size

The effect of the population size on hybrid CGA/PSO is investigated by varying the size from 4 to 40. The numerical results are recorded in Table 5 with the relevant graph plotted in Fig. 4, showing the average iteration, average time and the success rate obtained. From this graph, a larger population size contributes to results with higher success rate. However, the drawback of higher population size is the increment of the computational cost, as can be observed from the graph.

From Fig. 4 the curve of success rate seems to reach a stable stage with a specific population size. Hereby, we name this as "stable population size". For the IEEE 118-bus system in Fig. 4, the adopted population size is 16, the point given by the crossover point of the iteration and time curves in the figure. The same analysis is performed for other test systems with the preferred population sizes summarized in Table 6. It can be observed that for small systems, a small population size of 8 is enough. When the system size is higher than 30 buses, the population size increases and for a large system more then 118 buses, size 16 or more is needed.

6.3 Mutation Probability (*mp*)

This mutation rate denotes the degree of contribution from PSO algorithm for efficient search as this is implemented as mutation in the proposed hybrid CGA/PSO algorithm. The parameter sensitivity analysis for *mp* is carried out to find the best value for the best performance of the proposed hybrid method. The mutation probability, *mp* is set from 0.1 to 1.0 with step increment size of 0.1 in parameter sensitivity analysis. Results are shown in Table 7 with the relevant graphs in Fig. 5 for the case of the IEEE 118-bus test system. From the table, the best *mp* value is 1.0 when the mean iteration

is 6.1 within 3.07s. The success rate recorded in this case is 94%, which is the highest among all the *mp* values, highlighted in Table 7. The graph showing the relevant information versus the mutation probability *mp* is shown in Fig. 5.

As different power systems may exhibit different behaviour, therefore, the similar parameter analysis as in Table 7 is carried out for other systems to obtain the appropriate value of mutation probability for each system in the aim of obtaining optimal performance. The best values obtained for other IEEE test systems are summarized in Table 8 below. It can be observed, a setting of 0.4 suffices for small systems and 1.0 for larger systems.

7 Application Studies

In validating the hybrid CGA/PSO algorithm for finding the load flow solution of power systems under the heavy load condition and to compare its performance with ACGA, the following test systems and load variations have been used:

1. IEEE 30-bus system with load increment from 52.86% to 53.09% of normal loading
2. IEEE 57-bus system with load increment from 40.78% to 40.86% of normal loading
3. IEEE 118-bus system with load increment from 61.37% to 61.40% of normal loading

The best parameter settings summarised in Tables 4, 6 and 8 have been applied to the proposed hybrid method. To investigate the effects of population size, for each system, two extra population sizes of 50 and 100 have also been employed. The algorithms have been run for 50 trials in each case. The study results are summarized in Tables 9-11. At 52.86%, 40.78% and 61.37% load increment points respectively for the 30-bus, 57-bus and 118-bus IEEE test systems, the success rate in obtaining the load flow solutions by the proposed hybrid CGA/PSO algorithm is 100% for all the population sizes considered.

For the IEEE 30-bus system, it is observed from Table 9 that the hybrid CGA/PSO has a much higher success rate for finding the load flow solution when compared to ACGA for all the load increment points from 52.86% to 53.09%. For instance, the success rate of the hybrid CGA/PSO for the 52.86%, 52.89 and 52.92% load increment points are very close to 100%. The respective success rates recorded by the ACGA method are not satisfactory. The higher success rate obtained by the hybrid CGA/PSO signifies that the new algorithm has a much better performance than ACGA. Further

more, the ACGA can no longer find anymore solutions beyond 53.04% load increment. However, the hybrid CGA/PSO can still find solutions with success rates between 52% to 18%, even under a small population size of 8, just before the 53.09% load increment point, after which point there are no more feasible solutions. From the comparison of the execution times listed in Table 9, it can be observed that the hybrid CGA/PSO is much faster than ACGA. The voltage profiles of IEEE 30-bus system for 52.86% and 53.09% load increments are shown in Table 12. All the PV nodes, as highlighted in Table 12 are converted to PQ nodes when the reactive power limits are reached.

For the case of IEEE 57-bus system, from the results in Table 10, similar conclusions as that for the case of the 30-bus system can be derived. For the case of IEEE 118-bus system; from Table 11, it can be observed that at the loading point of 61.37% load increment, the proposed hybrid CGA/PSO algorithm obtained the solution with 100% success rate despite the small population size of 16. On the other hand, the ACGA algorithm found the solution for the same loading point with a much lower success rate of 56%. For further load increment up to 61.40%, ACGA failed to find the solution but the proposed hybrid algorithm can still find the solution although the success rate is low. This indicates the proposed algorithm is much more powerful than ACGA. There are no more solutions present beyond the loading point of 61.40% of load increment. The voltage profile of the 54 generator nodes of the 118-bus test system at 61.37% load increment are tabulated in Table 13. The variation of voltage with active power from normal load to 61.37% load increment for node 118 is illustrated in Fig. 6.

For all the test cases, from Table 9 to Table 11, the effect of increasing the population sizes in the proposed hybrid CGA/PSO algorithm is that the computing time is also increased. However, the number of iterations taken by the algorithm does not necessarily increased when the population size becomes larger.

Taking the maximum loading points (MLP) of the test systems to be the highest loading points found by the ACGA, the proposed hybrid algorithm with 100% success rate and the Newton Raphson method, the MLPs of the test systems found are tabulated in Table 14. The MLPs found by the hybrid CGA/PSO are higher than those by ACGA especially those for the 118-bus test system and are in close agreement with those found by the Newton-Raphson method. The improvement is due to the replacement of the nodal voltage differential acceleration technique in ACGA by PSO in forming the hybrid CGA/PSO algorithm.

It is worthwhile to recall that conventional methods based on Newton type of approach are greatly influenced by the initial setting of the nodal voltage values and they often encounter convergence problem at extremely heavy loading situations where the solution is at the vicinity of the MLP point. As shown by the above results, both these disadvantages of the conventional methods do not present in the proposed algorithm. Furthermore, while the solution acceleration techniques in ACGA reported to the earlier work [16] has improved the CGA loadflow algorithm in [15] greatly, the use of PSO in place of the nodal voltage differential acceleration technique in ACGA provides an even more powerful algorithm. This is because the PSO can create a more diversified population of candidate solutions through the acceleration of the current candidate solution towards the *gbest* and *pbest* solutions in the population. Furthermore, unlike the conventional methods, PSO does not require any gradient information.

8 Conclusions

A hybrid CGA/PSO algorithm has been developed based on the earlier constrained genetic algorithm for solving the load flow problem. Through its applications to three IEEE test systems, the hybrid algorithm has been found to be much more powerful and efficient than the previous ACGA algorithm particularly when it is applied to evaluate the load flow solution of heavy-loaded power systems. The large capability of the proposed algorithm allows it to evaluate the maximum loading points with better accuracy for larger systems than ACGA. The paper also reported the experimental determination of the best values of the parameters for use in the PSO part of the hybrid algorithm. The developed algorithm provides a very useful starting point for further development of tools for solving the heavy-loaded power systems containing nonlinear devices such as FACTS.

9 Acknowledgments

T.O. Ting wishes to express his gratitude to The Hong Kong Polytechnic University for providing him an International Postgraduate Scholarship to pursue postgraduate studies at the University. The authors are grateful to Dr An Li for his valuable discussions in the subject matter of the paper.

.

10 References

[1] Alvarado, F.L., Dobson, I, Thomas, R.J., and Hu, Y.: ‘Computation of closest bifurcation in power systems’, *IEEE Trans. Power Syst*., 1994, 9, (2), pp. 918-928

[2] Dobson, I.: 'Observations on the geometry of saddle node bifurcations and voltage collapse in electrical power systems', *IEEE Trans. Circuits and Syst.*-I, 1992, 39, (3), pp. 240-243

[3] Salam, F.M.A., Ni., L, Guo, S., and Sun, X.: 'Parallel processing for the load flow of power systems: the approach and applications'. Proc. 28th Circuits Devices Conf., Tampa, FL, Dec 1989, pp. 2173-2178

[4] Ma, W., and Thorp, J.S.: 'An efficient algorithm to locate all the load flow solutions', *IEEE Trans. Power Syst*., 1993, 8, (3), pp. 1077-1083

[5] Overbye, T.J., Demarco, C.L.: 'Improved technique for power system voltage stability assessment using energy methods', *IEEE Trans. on Power Syst.*, 1991, 6, (4), pp. 1496-1452

[6] Zarete, L.A.L, and Carlos, C.A., Ramos, J.M., and Ramos, E.R.: 'Fast computation of voltage stability security margins using nonlinear programming techniques', *IEEE Trans. Power Syst*., 2006, 21, (1), pp. 19-27

[7] Zarete, L.A.L, and Carlos, C.A.: 'Fast computation of security margins to voltage collapse based on sensitivity analysis', *IEE Proc. Gener. Transm. Distrib*., 2006, 153, (1), pp. 19-26

[8] Löof, P.-A, Andersson, G., and Hill, D.J.: 'Voltage stability indices for stressed power systems', *IEEE Trans. Power Syst*., 1993, 8, (1), pp. 326-335

[9] Cãnizares, C., Souza, A.C.Z., and Quintana, V.: 'Comparison of performance indices for detection of proximity to voltage collapse', *IEEE Trans. Power Syst*., 1996, 11, (3), pp. 1441-1450

[10] Zeng, Z.C., Galiana, F.D., Ooi, B.T., and Yorino, N.: 'A simplified approach to estimate maximum loading conditions', *IEEE Trans. on Power Syst.*, 1993, 8, (2), pp. 646-654

[11] Ajjarapu, V., and Christy, C.: 'The continuation power flow: a tool for steady state voltage stability analysis', *IEEE Trans. Power Syst.*, 1992, 7, (1), pp. 416-423

[12] Tinney, W.F., and Hart, C.E.: 'Power flow solution by Newton's method', *IEEE Trans. Power App. Syst*., 1967, PAS-86, pp.1449-1460

[13] Stott, B., and Alsac, O. 'Fast decoupled load-flow', *IEEE Trans. Power App. Syst.*, 1974, PAS-93, pp. 859-869

[14] Braz, L.M.C., Castro, C.A., and, Murari, C.A.F.: 'A critical evaluation of step size optimization based load flow methods', *IEEE Trans. Power Syst*., 2000, 15, (1), pp. 202-207

[15] Wong, K.P., Li, A., and Law, M.Y.: 'Development of constrained-genetic-algorithm load-flow method', *IEE Proc. Gener. Transm. Distrib.*, 1997, 144, (2), pp. 91-99.

[16] Wong, K.P., Li, A., and Law, T.M.Y.: 'Advanced constrained genetic algorithm load flow method', *IEE Proc. Gener. Transm. Distrib.*, 1999, 146, (6), pp. 609-616

[17] Kennedy, J., and Eberhart, R.C.: 'Particle swarm optimization', in Proc. IEEE Int. Conf. Neural Netw., 1995, pp. 1942-1948

[18] Huang, C.-M., Huang, C.-J., and Wang, M.-L.: 'A particle swarm optimization to identifying the ARMAX model for short-term load forecasting', *IEEE Trans. Power Syst.*, 2005, 20, (2), pp. 1126-1133

[19] Zhao, B., Guo, C.X., and Cao, Y.J.: 'A multiagent-based particle swarm optimization approach for optimal reactive power dispatch', *IEEE Trans. Power Syst.*, 2005, 20, (2), pp. 1070-1078

[20] Park, J.-B., Lee, K.-S., Shin, J.-R., and Lee K.Y.: 'A particle swarm optimization for economic dispatch with nonsmooth cost functions', *IEEE Trans. Power Syst.*, 2005, 20, (1), pp. 34-42

[21] Abido, M.A.: 'Optimal design of power-system stabilizers using particle swarm optimization', *IEEE Trans. Energ. Conv.*, 2002, 17, (3), pp. 406-413

[22] Shi, Y., and Eberhart, R.C.: 'A modified particle swarm optimizer', in Proc. IEEE Int. Conf. Evol. Comput., Anchorage, Alaska, 1998. pp. 69-73

[23] Clerc, M., and Kennedy, J.: 'The particle swarm: explosion, stability, and convergence in a multi-dimensional complex space', *IEEE Trans. Evol. Comput*., 2002, 6, (1), pp. 58-73

[24] Chatterjee, A., Pulasinghe, K., Watanabe, K., and Izumi, K. Izumi.: 'A particle-swarm-optimized fuzzy-neural network for voice-controlled robot systems', *IEEE Trans. on Industrial Electronics.,* 52, (6), pp. 1478-1489

[25] Power Systems Test Case Archive, University of Washington College of Engineering. [Online]. Available: http://www.ee.washington.edu/research/pstca/ , accessed on May 2006.

[26] Ting, T.O., Wong, K.P., Chung, C.Y.: 'Two-phase particle swarm optimization for load flow analysis,' Proc. 2006 International Conference on Systems, Man and Cybernetics (SMC 2006), Taipei, Taiwan, 8-11 October 2006, vol 1, pp. 2345–2350.

[27] Ting, T.O., Wong, K.P., Chung, C.Y.: 'Locating type-1 load flow solutions using hybrid evolutionary algorithm,' Proc. of the 5th IEEE International Conference on Machine Learning and Cybernetics (ICMLC 2006), Dalian, China, 13-16 August 2006, vol 7, pp. 4093-4098.

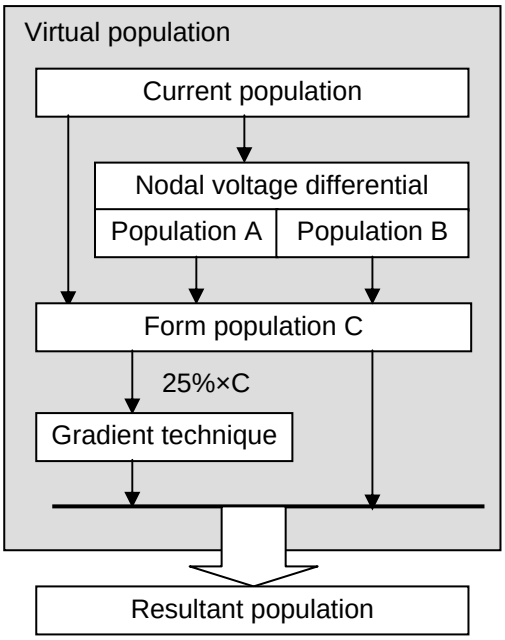

Fig. 1 Formation of virtual and resultant populations of candidate solutions in ACGA

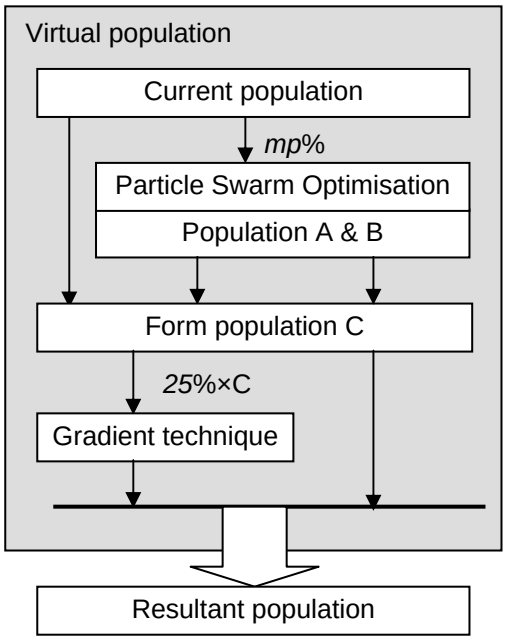

Fig. 2 The proposed framework showing the formation of virtual and resultant populations of candidate solutions

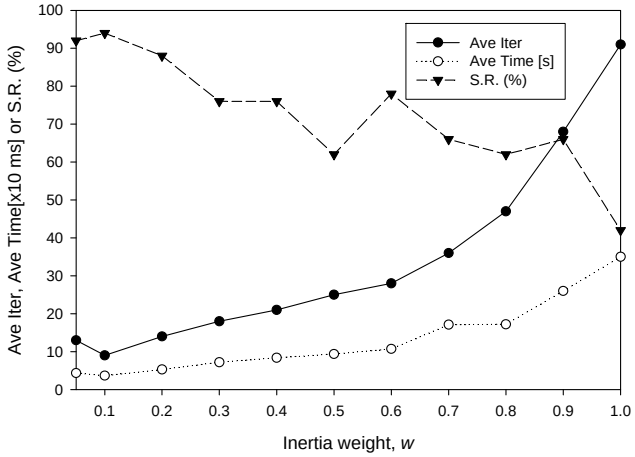

Fig. 3 Effects of inertia weight w (0.1 to 1.0): case of IEEE 118-bus system with 160% of normal load.

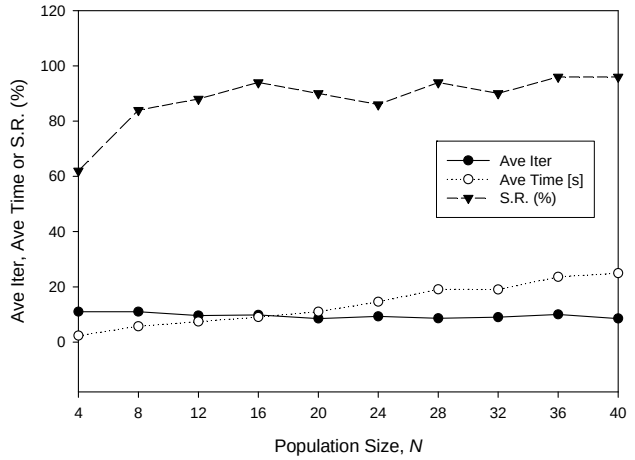

Fig. 4 Effect of population size N: case of IEEE 118-bus system with 160% of normal load.

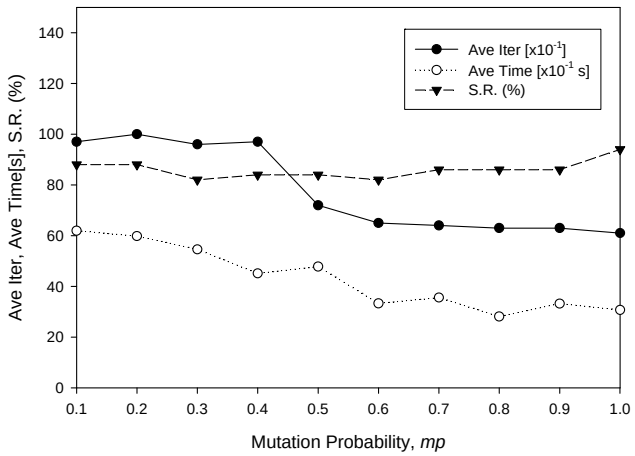

Fig. 5 Effect of mutation probability (*mp*): case of IEEE 118-bus system with 160% of normal load.

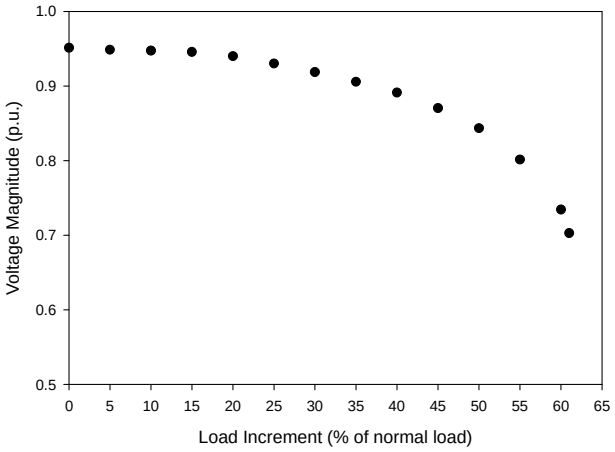

Fig. 6 Variation of nodal voltage magnitude with load increment at node number 118

Table 1: Common parameter settings for ACGA and Hybrid CGA/PSO

Parameter	Settings
Active and reactive power tolerance	0.001 p.u. on 100MVA base
Gradient acceleration, G	25% of the population
Number of trials	50
Maximum Generation, T	150
Voltage initialization range	$0.9 < V < 1.2$ and $-30° < \theta < 0°$
Population size, N	8

Table 2: Other parameter settings for ACGA and Hybrid CGA/PSO

Parameter	ACGA	Hybrid CGA/PSO
Crossover rate	Two-point crossover	Two-point crossover
Selection strategy	Roulette Wheel	Roulette Wheel
Mutation, mp	Uniform mutation with $mp = 0.01$	PSO mutation with $mp = 0.5$
Inertia weight, w	-	0.1
Maximum Velocity, V_{max}	-	10% of search space

Table 3: Parameter sensitivity analysis for inertia weight (w) with 60% load increment on IEEE 118-bus system

w	Ave Iter	Ave Time[s]	S.R. (%)	Std Dev	H		
					Best	Average	Worst
0.05	13	4.32	92	1.26×10^{-6}	0	1.08×10^{-6}	4.0×10^{-6}
0.1	**9**	**3.64**	**94**	$\mathbf{1.15\times10^{-6}}$	**0**	$\mathbf{1.06\times10^{-6}}$	$\mathbf{5.0\times10^{-6}}$
0.2	14	5.26	88	1.10×10^{-6}	0	1.11×10^{-6}	4.0×10^{-6}
0.3	18	7.18	76	9.35×10^{-7}	0	1.13×10^{-6}	3.0×10^{-6}
0.4	21	8.35	62	1.21×10^{-6}	0	1.26×10^{-6}	4.0×10^{-6}
0.5	25	9.37	62	1.36×10^{-6}	0	1.23×10^{-6}	5.0×10^{-6}
0.6	28	10.7	78	1.36×10^{-6}	0	1.80×10^{-6}	6.0×10^{-6}
0.7	36	17.1	66	1.41×10^{-6}	0	1.76×10^{-6}	6.0×10^{-6}
0.8	47	17.2	62	1.51×10^{-6}	0	1.68×10^{-6}	6.0×10^{-6}
0.9	68	26.1	66	1.36×10^{-6}	0	1.33×10^{-6}	5.0×10^{-6}
1.0	91	35.0	42	1.80×10^{-6}	0	2.57×10^{-6}	6.0×10^{-6}

Table 4: Inertia weight (w) obtained via parameter sensitivity analysis

System	IEEE 30-bus	IEEE 57-bus	IEEE 118-bus
w	0.1	0.1	0.1

Table 5: Parameter sensitivity analysis for population size N with 60% load increment on IEEE 118-bus system

N	Ave Iter	Ave Time[s]	S.R. (%)	Std Dev	H		
					Best	Average	Worst
4	11.0	2.34	62	1.63×10^{-6}	0	1.39×10^{-6}	7.0×10^{-6}
8	11.0	5.70	84	1.31×10^{-6}	0	1.19×10^{-6}	6.0×10^{-6}
12	9.6	7.41	88	1.28×10^{-6}	0	1.27×10^{-6}	5.0×10^{-6}
16	**9.8**	**9.07**	**94**	$\mathbf{1.30\times10^{-6}}$	**0**	$\mathbf{1.13\times10^{-6}}$	$\mathbf{6.0\times10^{-6}}$
20	8.5	11.0	90	1.02×10^{-6}	0	1.33×10^{-6}	4.0×10^{-6}
24	9.3	14.6	86	8.15×10^{-7}	0	9.53×10^{-7}	2.0×10^{-6}
28	8.6	19.1	94	1.20×10^{-6}	0	9.57×10^{-7}	5.0×10^{-6}
32	9.0	19.0	90	9.41×10^{-7}	0	1.02×10^{-6}	3.0×10^{-6}
36	10.0	23.6	96	1.33×10^{-6}	0	9.38×10^{-7}	6.0×10^{-6}
40	8.5	24.9	96	1.03×10^{-6}	0	1.15×10^{-6}	3.0×10^{-6}

Table 6: Stable population size obtained via parameter sensitivity analysis

System	IEEE 30-bus	IEEE 57-bus	IEEE 118-bus
N	8	12	16

Table 7: Parameter sensitivity analysis for mutation probability (*mp*) with 60% load increment on IEEE 118-bus system (50 Trials)

mp	Ave Iter	Ave Time[s]	S.R. (%)	Std Dev	H		
					Best	Average	Worst
0.1	9.7	6.19	88	1.06×10^{-6}	0	1.00×10^{-5}	5.0×10^{-6}
0.2	10	5.98	88	1.50×10^{-6}	0	1.48×10^{-6}	7.0×10^{-6}
0.3	9.6	5.46	82	1.42×10^{-6}	0	1.32×10^{-6}	5.0×10^{-6}
0.4	9.7	4.51	84	5.84×10^{-6}	0	1.88×10^{-6}	3.8×10^{-5}
0.5	7.2	4.78	84	1.45×10^{-6}	0	1.19×10^{-6}	5.0×10^{-6}
0.6	6.5	3.33	82	1.08×10^{-6}	0	1.22×10^{-6}	5.0×10^{-6}
0.7	6.4	3.56	86	7.83×10^{-7}	0	6.51×10^{-7}	3.0×10^{-6}
0.8	6.3	2.81	86	3.24×10^{-7}	0	1.16×10^{-7}	1.0×10^{-6}
0.9	6.3	3.32	86	1.52×10^{-7}	0	2.33×10^{-8}	1.0×10^{-6}
1.0	**6.1**	**3.07**	**94**	$\mathbf{5.83\times10^{-7}}$	**0**	$\mathbf{8.51\times10^{-8}}$	$\mathbf{4.0\times10^{-6}}$

Table 8: Mutation probability (*mp*) obtained via parameter sensitivity analysis

System	IEEE 30-bus	IEEE 57-bus	IEEE 118-bus
mp	0.4	0.4	1.0

Table 9: Performances of algorithms for the case of IEEE 30-bus system

Load Inc (%)		52.86			52.89			52.92			52.95			52.98			53.01			53.04			53.07			53.09		
Population size		8	50	100	8	50	100	8	50	100	8	50	100	8	50	100	8	50	100	8	50	100	8	50	100	8	50	100
ACGA	S.R(%)	28	86	94	26	52	100	12	40	76	6	30	57	2	26	42	0	16	20	0	0	4	0	0	0	0	0	0
	Ave Iter	48	27	32	118	48	52	141	65	46	67	52	47	78	35	45	-	92	68	-	-	94	-	-	-	-	-	-
	Time[s]	0.41	2.4	3.7	0.8	4.0	9.2	1.0	5.2	8.9	0.6	4.0	7.9	0.7	4.9	8.4	-	12.7	17.6	-	-	21.1	-	-	-	-	-	-
Hybrid CGA/PSO	S.R(%)	100	100	100	90	92	100	96	98	100	32	48	68	86	94	100	52	84	94	42	56	67	18	26	30	4	2	6
	Ave Iter	26	24	22	49	52	35	32	43	30	30	35	29	43	38	35	54	83	62	64	115	96	73	62	56	79	125	3
	Time[s]	0.28	2.1	3.2	0.65	4.3	7.6	0.36	4.1	7.4	0.34	3.6	6.8	0.52	4.1	7.3	0.6	9.2	15.6	0.7	10.9	17.5	0.8	7.5	13.2	0.9	16.7	23.4

Table 10: Performances of algorithms for the case of IEEE 57-bus system

Load Inc(%)		40.78			40.79			40.80			40.81			40.82			40.83			40.84			40.85			40.86		
Population size		12	50	100	12	50	100	12	50	100	12	50	100	12	50	100	12	50	100	12	50	100	12	50	100	12	50	100
ACGA	S.R(%)	92	98	100	60	64	100	68	76	100	18	36	68	0	24	36	0	0	12	0	0	8	0	0	4	0	0	0
	Ave Iter	6	5	5	36	6	5	46	6	6	79	24	19	-	24	17	-	-	43	-	-	37	-	-	51	-	-	-
	Time[s]	0.75	2.8	5.5	1.5	4.7	8.6	2.8	3.1	5.9	4.1	7.1	18.2	-	6.8	11.3	-	-	22.3	-	-	20.1	-	-	26.3	-	-	-
Hybrid CGA/PSO	S.R(%)	100	100	100	90	88	100	76	82	100	32	72	80	24	48	50	16	32	46	6	20	34	2	12	23	0	4	8
	Ave Iter	6	5	5	15	7	6	20	8	8	42	16	23	33	18	23	36	23	21	36	35	29	52	40	45	-	48	39
	Time[s]	0.6	2.5	5.3	1.1	2.9	5.7	1.5	3.3	6.5	3.4	5.8	12.1	2.1	6.2	12.3	2.3	6.7	11.2	2.2	8.2	13.6	3.1	9.8	21.2	-	11.7	19.6

Table 11: Performances of algorithms for the case of IEEE 118-bus system

Load Inc (%)		61.37			61.38			61.39			61.40		
Population size		16	50	100	16	50	100	16	50	100	16	50	100
ACGA	S.R (%)	56	72	100	48	54	76	32	26	54	0	0	0
	Ave Iter	11	7	7	12	8	7	14	9	7	-	-	-
	Time[s]	16.4	39.1	74.4	17.4	43.5	85.4	19.3	42.7	87.2	-	-	-
Hybrid CGA/PSO	S.R (%)	100	100	100	92	90	100	48	72	96	0	2	6
	Ave Iter	7.1	7.0	7.1	7.6	7.2	7.1	8.9	7.2	7.0	-	15.6	15.1
	Time[s]	9.6	30.9	64.7	10.3	31.4	62.5	10.7	32.4	63.3	-	131.5	256.1

Table 12: Voltage profiles of IEEE 30-bus system under two heavy load conditions

Load	52.86% load increment		53.09% load increment	
Node No.	Magnitude (pu)	Angle (deg)	Magnitude (pu)	Angle (deg)
1	1.060000	0.000000	1.060000	0.000000
2	**0.902526**	**-9.163226**	**0.898054**	**-9.193436**
3	0.825449	-14.144292	0.818886	-14.224428
4	0.779957	-17.714087	0.772084	-17.843672
5	**0.744227**	**-30.230791**	**0.735514**	**-30.673100**
6	0.746917	-21.817823	0.737926	-22.027609
7	0.726796	-26.740196	0.717579	-27.084412
8	**0.734867**	**-23.712009**	**0.725587**	**-23.968462**
9	0.737971	-30.984142	0.726524	-31.451153
10	0.699372	-36.278351	0.686610	-36.930237
11	**0.800427**	**-30.968399**	**0.789912**	**-31.432629**
12	0.743886	-34.378109	0.732089	-34.962929
13	**0.786679**	**-34.370037**	**0.775517**	**-34.952236**
14	0.706474	-37.226383	0.693927	-37.909386
15	0.692698	-37.416431	0.679860	-38.100208
16	0.708628	-36.032516	0.696212	-36.673157
17	0.689950	-36.905891	0.677058	-37.581543
18	0.665953	-39.475880	0.652561	-40.231888
19	0.657619	-40.039063	0.644044	-40.821728
20	0.666093	-39.276268	0.652661	-40.027641
21	0.669230	-37.823486	0.655811	-38.533367
22	0.670242	-37.767101	0.656822	-38.473484
23	0.661392	-38.628609	0.647855	-39.358040
24	0.639610	-39.044552	0.625182	-39.806389
25	0.641373	-38.172943	0.626557	-38.930454
26	0.596671	-39.874516	0.580452	-40.735943
27	0.664258	-36.653721	0.650009	-37.369335
28	0.727160	-23.398275	0.717403	-23.637709
29	0.609867	-41.403164	0.593751	-42.335968
30	0.578284	-45.204037	0.561152	-46.372238

Table 13: Voltage profile of generator nodes for IEEE 118-bus system with 61.37% load increment

Node No.	Mag (pu)	Ang (deg)	Node No.	Mag (pu)	Ang (deg)	Node No.	Mag (pu)	Ang (deg)
1	0.9189	-96.67	42	0.9850	-72.50	80	0.9387	-10.92
4	0.9980	-89.12	46	0.8376	-40.58	85	0.9282	-26.13
6	0.9760	-92.65	49	0.8725	-34.67	87	1.0150	-29.12
8	1.0150	-80.67	54	0.9251	-48.90	89	1.0050	-21.28
10	1.0500	-65.84	55	0.9115	-49.04	90	0.9850	-29.22
12	0.9144	-93.58	56	0.9130	-48.79	91	0.9800	-28.60
15	0.9091	-89.41	59	0.9441	-38.65	92	0.9616	-26.58
18	0.9189	-88.78	61	0.9950	-28.56	99	0.9961	-27.64
19	0.8977	-88.91	62	0.9809	-29.35	100	0.9573	-30.84
24	0.9920	-61.83	65	0.9205	-13.78	103	0.9389	-38.21
25	1.0500	-65.70	66	0.9788	-20.64	104	0.9158	-43.20
26	1.0150	-64.38	69	1.0350	30.00	105	0.9193	-45.31
27	0.9680	-83.61	70	0.7297	-11.84	107	0.9520	-50.57
31	0.9670	-87.68	72	0.9222	-44.96	110	0.9533	-50.02
32	0.9604	-83.62	73	0.8311	-20.20	111	0.9800	-48.69
34	0.8521	-77.98	74	0.6798	-10.65	112	0.9750	-54.37
36	0.8457	-78.93	76	0.6791	-15.25	113	0.9930	-86.03
40	0.9700	-80.41	77	0.8465	-8.99	116	1.0050	-3.05

Table 14: Comparison of Maximum Loading Point (MLP)

System	MLP (% of Increment from normal load)	
	ACGA	Hybrid CGA/PSO
IEEE 30-bus	52.23	52.86
IEEE 57-bus	40.70	40.78
IEEE 118-bus	60.70	61.37